1 Technical Overview

1.1 Background

The CCAT science case, observatory requirements, and conceptual design were developed as part of a $2M study jointly funded by Cornell and Caltech/JPL, which resulted in a Feasibility/Concept Design Study Report[2] that was completed and reviewed[16] in January 2006. The primary goal was to define a facility whose scientific capability would represent a substantial advance over the present generation of $10-15\,$m class submillimeter telescopes, and which, unlike most existing mm/submm telescopes, would be designed from the start for a very wide field of view in order to exploit the rapid ongoing development of submillimeter detector array technology. It was recognized that in order to make best use of the nation's substantial investment in ALMA, the US astronomical community would need access to an instrument located in the southern hemisphere capable of making rapid wide-field surveys with a flux sensitivity sensitivity comparable to ALMA.

1.2 General Characteristics

The overall specifications for the CCAT observatory are listed in Table 1, reproduced from Section 5.1 of the CCAT Feasibility Study report[2]. These specifications were derived by considering a broad spectrum of science programs ranging from studies of trans-Neptunian objects in the outer solar system to surveys for high-redshift submillimeter galaxies. Commonly recurring themes included the desire for high sensitivity approaching that of ALMA, the need for good angular resolution to overcome spatial confusion, and a wide wavelength coverage in order to constrain the spectra and luminosities of dusty objects. These considerations led to the choice of a 25 m telescope with a 20' field of view, a half-wavefront error (HWFE) around $10\,\mu$m rms for high aperture efficiency at 350 μm, and a location on a high (5600 m) mountain site in Atacama above the Chajnantor plateau for routine access to the 350 μm atmospheric window.

Figure 1: Left: A view of Cerro Chajnantor from the Chajnantor plateau. The summit road constructed by U. Tokyo is visible. Right: A view of the CCAT test instrumentation at the proposed proposed site.

Table 1: CCAT Specifications

Specification	Requirement	Goal	Remarks
Aperture	25 m		sensitivity, confusion
Wavelength range	$350 - 1400\,\mu$m	$200 - 3500\ \mu$m	dust SED
Field of view	10'	20'	large-format arrays
Angular resolution	3".5–14"	2"–35"	$\theta = 1" \times \lambda/(100\,\mu\text{m})$
Half Wavefront Error	$< 12.5\ \mu$m	$< 9.5\ \mu$m	rms (HWFE)
Site conditions	< 1 mm	< 0.7 mm	median pwv
Polarization	0.2%	0.05%	after calibration
Emissivity	$< 10\%$, $\lambda > 300\ \mu$m	$< 5\%$, $\lambda > 800\,\mu$m	sky loading is low
	$< 20\%$, $\lambda = 200\ \mu$m		
Elevation range	$5 - 90°$		from horizon
Azimuth range	±270°		from north
Pointing, blind	2"	0".5	rms
offset	0".3	0".2	within 1°
repeatability	0".3	0".2	rms, one hour
Scan rate	$0°.2\ \text{s}^{-1}$	$1°\ \text{s}^{-1}$	slow and fast modes
acceleration	$0°.4\ \text{s}^{-2}$	$2°\ \text{s}^{-2}$	efficient scan patterns
pointing knowledge	0".2	0".1	rms
Secondary nutation	±2'.5		@ 1Hz, azimuth only

1.3 Proposed Site

The proposed site for CCAT is at an altitude of 5612 m, on a plateau about 50 m below and 200 m east-north-east of the summit of Cerro Chajnantor (Fig. 1), within the Science Preserve established by the Chilean Government. This selection was made after considering several alternative locations nearby, including Cerro Negro at a somewhat lower 5000 m altitude. With permission from CONICYT, site testing equipment was deployed on Cerro Chajnantor in 2006 May, including a $350\,\mu$m tipping radiometer that previously had been cross-compared to an identical unit operating at the CBI site on the Chajnantor (ALMA) plateau. Results[13] from simultaneous $350\,\mu$m measurements using the two instruments on the summit and plateau demonstrate that Cerro Chajnantor is indeed an excellent submillimeter site, significantly superior to the Chajnantor plateau, with a $350\,\mu$m opacity ratio of around 0.6–0.7 between the two locations. This conclusion is supported by meteorological data gathered at the two sites that demonstrate that the water vapor density is significantly lower on the summit. This opacity advantage can be quantified in terms of observing time: relative to the plateau, the CCAT site offers nearly twice as much high-quality observing time in the crucial $350/450\,\mu$m atmospheric windows.[2]

1.4 Sensitivity

Multiple factors – the 25 m aperture, the improved atmospheric transparency of the higher site, the use of broadband continuum detectors instead of narrowband heterodyne receivers, the high aperture efficiency resulting from a $\sim 10\,\mu$m rms surface, and the possibility of achieving sensitivities limited by photon statistics and not by (heterodyne) receiver noise – all combine to give CCAT a continuum point-source flux sensitivity in the 350 μm and

Table 2: CCAT Continuum Sensitivity

λ (μm)	ν (GHz)	PWV (mm)	NEFD[a] (mJy $s^{1/2}$)	CL flux[c] (mJy)	CL time[d] (min)	CL density[b] deg^{-2}	CL mapping[e] $deg^2\ yr^{-1}$
200	1500	0.3	150.96	0.356		115,935	
228	1317	0.3	116.67	0.529		89,409	
291	1030	0.3	114.17	0.926		54,677	
350	857	0.4	14.41	1.293	52	37,856	26
450	667	0.5	13.80	1.450	38	22,901	60
620	484	0.5	16.35	1.277	68	12,064	23
740	405	0.7	8.74	1.112	26	8,469	75
865	347	1.0	5.83	0.922	17	6,198	319
1100	273	1.0	2.06	0.670	3.9	3,833	1980
1180	254	1.0	1.74	0.610	3.4	3,325	2300
1400	214	1.5	2.93	0.447	18	2,366	436
2000	150	1.5	2.30	0.196	58	1,159	80
3300	90.9	1.5	2.82	0.080	513	426	9

[a] The NEFD is the $1\,\sigma$ flux sensitivity achieved for an integration time of one second, calculated using the appropriate precipitable water vapor (PWV), as listed.

[b] The source density at the confusion limit (CL) is taken to correspond to 30 beams per source. For reference, deep 24 μm imaging with Spitzer[12] yields $N(S_{24\,\mu\rm m} > 30\,\mu\rm Jy) \approx 60,000\ \rm deg^{-2}$.

[c] The source flux density level reached at the confusion limit (model prediction).

[d] The time required to reach the confusion-limited flux, calculated for $5\,\sigma$ detection.

[e] The confusion–limited mapping speed, taking into account PWV statistics (see Table 3), for a PWV-scheduled observing program utilizing instruments with $50,000$ detectors.

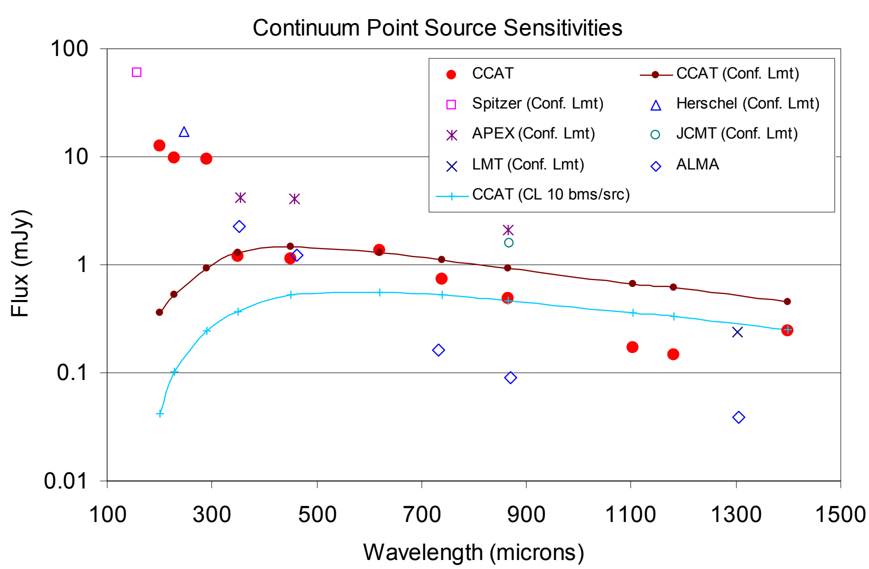

Figure 2: CCAT continuum point-source sensitivity compared to other facilities, calculated for a 5σ detection in a one hour integration.

450 μm atmospheric windows that is comparable to ALMA on a per-pixel basis. Therefore, with the use of large array cameras, the mapping speed for CCAT will be many orders of magnitude faster than ALMA, allowing CCAT to serve as an effective survey instrument to complement ALMA.

The predicted sensitivity for CCAT is shown in Table 2; the corresponding details may be found in the Feasibility Report.[2] For deep imaging, the raw sensitivity (NEFD) must be supplemented by estimates of the source confusion limit. Because CCAT's sensitivity and angular resolution will allow us to probe much more deeply into the submillimeter galaxy population than current instruments, the confusion limit is not yet known and must be predicted using models[4] that basically extrapolate existing (shallower) measurements. At $\lambda = 350\,\mathrm{um}$, and using a conservative value of 30 beams per source, CCAT's angular resolution of 3".5 yields a confusion-limited areal density around 40,000 sources per square degree, which is quite comparable to deep 24 μm counts with Spitzer.[12] Fig. 2 shows that CCAT and ALMA should have comparable sensitivities at 350 and 450 μm, with ALMA gaining a factor of ~ 10 advantage at long wavelengths. However, the use of large focal plane arrays makes CCAT's mapping speed several orders of magnitude faster than ALMA even at long wavelengths. Relative to existing 10-15 m telescopes, CCAT should be well over an order of magnitude faster to reach a given flux level, and has a deeper confusion limit. For spectroscopy, line flux sensitivities are given in the Feasibility Report[2] and lie in the range $2.2 \times 10^{-18}\,\mathrm{W\,m^{-2}}$ at $\lambda = 350\,\mu\mathrm{m}$ to $1.6 \times 10^{-19}\,\mathrm{W\,m^{-2}}$ at $\lambda = 1.2\,\mathrm{mm}$.

1.5 Infrastructure

Plans for development of CCAT have assumed that the existing infrastructure roads, radio communications, access control, and emergency management which currently exist will continue to be available. In some cases these capabilities are provided by partnership of the various projects underway in the Preserve, and CCAT, through participation in the Chajnantor Working Group is a partner in these efforts. The Project plan for CCAT includes provisions for joint funding of collaborative efforts between Projects. Like the other projects in the Science Preserve, CCAT will depend somewhat on the resources available in San Pedro de Atacama, Calama, Antofagasta, and other Chilean population centers. CCAT has established a relationship with Associated Universities Inc. (AUI) with a view towards employing the resources of AUI in Chile to support such activities as staffing, import/export, shipping, and some aspects of Chilean government relations. In return, AUI would be fully compensated for such activities by the CCAT partnership.

1.6 Construction

Construction of the CCAT observatory includes the following items:

1. **Road Improvements**: The access road on Cerro Chajnantor will be improved to provide access for the required construction materials and subassemblies and to provide safe transit consistent with regular operations. Preliminary discussions regarding coordination and cost-sharing have been held with the University of Tokyo's Institute of Astronomy.

2. **Utilities**: CCAT plans to be self sufficient, with electrical power to be provided by two 750 kVA diesel generators at the base of the summit access road.

3. **Base Facility**: CCAT has plans for the construction of a base facility in or near San Pedro de Atacama, similar in scope and tone to those of APEX. The facility is a dedicated group of buildings within a *recinto* which include dormitories, offices, a kitchen/dining room, and a warehouse.

4. **Telescope Facility**: The CCAT Telescope Facility on the summit is described in more detail in the Feasibility Report.[2] Construction is a typical metal building with concrete foundations, ring wall for dome support, and floors. The remainder of construction is steel framed with standard interior and exterior finishes.

   (a) **Dome**: CCAT will employ a Callotte type dome, 40 meters in diameter, which uses two rotational stages to achieve azimuth and elevation motions. Construction is steel frame with either steel, aluminum, or fiberglass cladding. Dome weight is of order 500 tons. This is a similar approach to that being taken by the Thirty Meter Telescope project. The Calotte, using a geodesic type structure, can be readily assembled at the challenging CCAT site.

   (b) **Telescope Mount**: Constructed of steel, the CCAT Mount is an altitude/elevation type mount using both hydrostatic and rolling element bearings, multiple drives, optical encoders, and offering Nasmyth and bent Cassegrain instrument locations. It weighs approximately 650 tons and is designed in modules for ease of transportation to the telescope site and simple on-site assembly.

   (c) **Primary Mirror**: The primary mirror of CCAT is made up of multiple mirror segments which mount via linear actuators to the primary mirror truss. The baseline design is a steel space frame of bolted construction; carbon-fiber options will also be reviewed. The truss is assembled on site without welding or adjustment and attaches to the telescope mount. Gravitational and thermal distortions of the primary mirror assembly are corrected using the segment actuators. Control of segment positions is closed–loop using data from distributed sensor systems.

   (d) **Mirror Segments, M2/M3**: Two alternative approaches to mirror segments are under development. One utilizes composite monolithic panels and the other uses multiple smaller panels on a support structure to make up larger, compound segments. M2/M3 are approximately 2.7 m in diameter (1.9m $\times$ 2.7 m for M3.) Mounting for M2 will include a hexapod for alignment and a nutator. The CCAT nutator is only slightly larger than that developed for the IRAM 30 m. M3 will be mounted to a turntable to allow the image to be directed to either Nasmyth instrument location or one of the two Bent Cassegrain positions also available.

While Cerro Chajnantor is certainly a challenging site for construction, this is offset somewhat by the ALMA experience and the demonstrated capabilities of Chilean construction companies to construct complex mining facilities at similar locations. The major subsystems will be designed with site assembly in mind. Field welding and alignment will be minimized and pre-shipment trial assembly will be emphasized. All workers on site will be required to use supplementary oxygen for both safety and efficiency.

2 Technology Drivers

2.1 Precision Active Surface

Figure 3 graphically illustrates the technical challenge of constructing a telescope according to CCAT's specifications. Of the total $\sim 10\,\mu$m rms half-wavefront error (HWFE), around 7 μm rms is allocated to the 25 m primary surface. This specification places CCAT well beyond the standard gravitational limits and approaches the thermal limits for the best materials such as CFRP. Consequently, an active surface is necessary, in which the reflector surface is segmented and the reflector segments are attached via actuators to the truss (back-up structure). The actuators are periodically adjusted to allow the deformations of the truss to be compensated, allowing the surface precision to be maintained. This approach is followed in other recently constructed large telescopes such as the 100 m GBT and the 50 m LMT. However, for those telescopes the active surface is generally operated "open–loop", typically using table look–up to correct for gravitational distortions. The GBT is currently experimenting with the use of out-of-focus holography using a bolometer camera in order to correct for large-scale thermal distortions every few hours.[9] Given the demanding requirements for CCAT, we have focused on a more rigorous closed–loop operating mode in which the actuator commands incorporate information from a distributed network of sensors, loosely modeled after the edge-sensor approach used by the Keck telescopes, but supplemented by angle sensors such as a Shack-Hartmann camera. In predicting the performance of the telescope, it is necessary to consider the thermal deformation properties of individual reflector segments and their size limitations in addition to the properties and performance of the sensor system. Thus, the choice of segment technology is a key issue. We are focusing on two options: CFRP monolithic panels, and compound panels (see Fig. 3); at present, both appear to lead to viable solutions for CCAT's active surface.[11, 17]

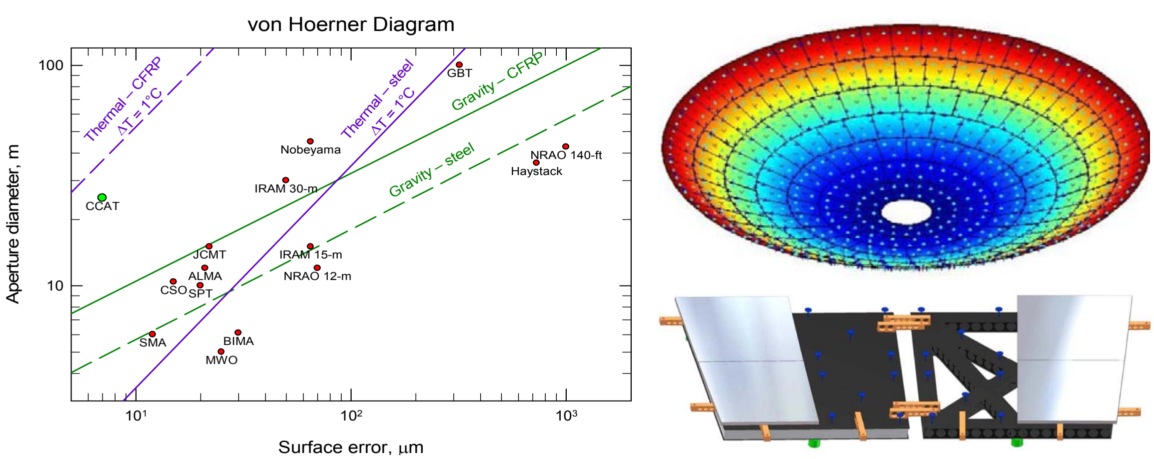

Figure 3: Left: Aperture vs. surface rms error, after von Hoerner.[15] The "gravity" and "thermal" lines illustrate limits for passive structures due to the physical properties of materials (steel and CFRP). Right, top: Baseline "keystone" segmentation with ~ 2 m panels, 210 panels total. Right, bottom: A "compound panel" utilizing smaller reflector tiles attached to a CFRP subframe to synthesize a larger segment. This approach allows segment sizes of order 3-4 m to be considered.

2.2 Imaging and Spectroscopic Instruments

The scientific power of CCAT derives from recent advances in submillimeter detector array technology. As shown in Figure 4, array sizes have been growing exponentially. At present, the state of the art is represented by the kilopixel-scale arrays of superconducting transition-edge sensor (TES) bolometers now in use at SPT and ACT. The SCUBA 2 instrument, in commissioning at the JCMT, also has roughly 1 kilopixels functioning at present, but ultimately will have 10^4 pixels once the science-grade arrays are installed. For CCAT, the goal is to have cameras with up to $\sim$ 50 kilopixels available at "first light".[1, 14] Two cameras are envisioned: a short-wavelength camera covering $200 - 620\,\mu$m, and a long–wavelength camera covering $740 - 2000\,\mu$m. With 50,000 Nyquist-sampled pixels, CCAT's field of view could be filled at $\lambda = 1$ mm. However, since the number of pixels required scales as λ^{-2}, filling the field of view at 350 μm would require of order 400 kilopixels. Clearly, building instruments at this scale presents a broad spectrum of technical challenges: the related cryogenics, optics, baffling, shielding, electronics, and mechanical issues must all be dealt with. These are long-term challenges: it is important to remember that CCAT can produce outstanding science even with existing kilopixel-scale arrays.

Similar challenges exist for spectroscopic instrumentation.[3] One goal is to construct broadband direct-detection grating spectrometers, capable of determining redshifts via the C^+ or CO lines. Existing examples include the Z-spec and ZEUS instruments now in use at the CSO. However, for CCAT we envision going beyond these single-beam instruments and building multi-object spectrometers, capable of observing 10–100 objects simultaneously while spanning multiple atmospheric windows. Again, this presents numerous technical challenges. It is now also becoming possible to construct large heterodyne array instruments for high-resolution spectral mapping. The 64-pixel 350 GHz system in construction at U. Arizona provides one example;[8] ultimately, systems with 256–1024 pixels should be possible.

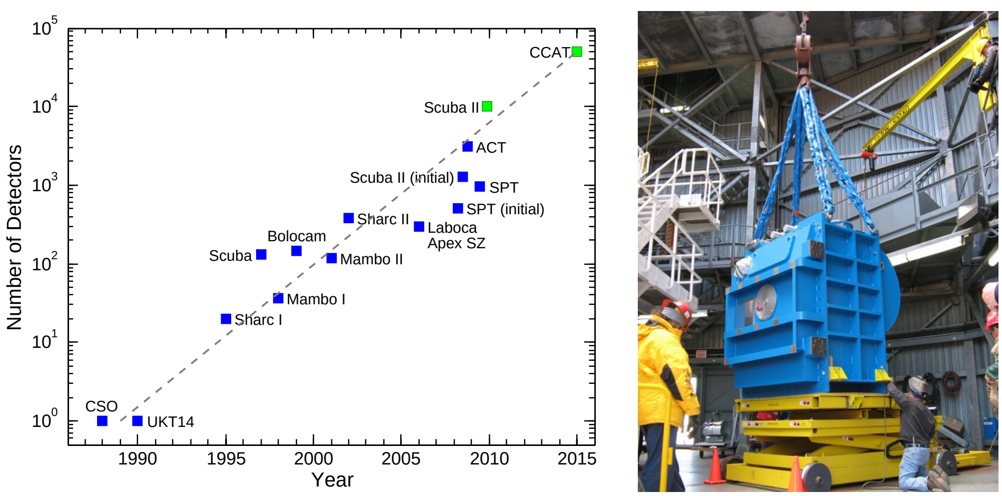

Figure 4: Left: The growth of mm/submm detector array size as a function of time has followed an exponential trend over the past two decades, with a growth rate exceeding a factor of 2 every two years. Blue points represent existing (or obsolete) instruments; the green points are projections. Right: The SCUBA 2 instrument arriving at the JCMT in early 2008.

2.3 Large-Format Submillimeter Detector Arrays

As shown in Fig. 4, the number of detector pixels in mm/submm instruments has been growing exponentially. Early single-pixel bolometer instruments, and JCMT's Scuba 1, used hand-assembled bolometers in which a germanium or silicon thermistor chip was attached to an absorbing substrate and was suspended from a metal frame using very thin leads. Readout was performed using individual low-noise JFET pre-amplifiers operated at ∼100 K, with leads for each pixel running from the cold stage to the JFETs. A major step forward was the introduction of lithographic fabrication,[7] which greatly reduces the labor needed to fabricate arrays. This technology was adopted for instruments such as CSO's Sharc 1 (20 pixels) and Bolocam (144 pixels). However, the readout scheme was the same, with individual JFET preamps and large numbers of leads.

The introduction of the superconducting transition edge sensor[10] (TES) as a replacement for semiconductor thermistors and the invention of multiplexed superconducting readouts [5, 18] reduced the lead counts and enabled kilopixel–scale arrays. The SCUBA 2 array is the most ambitious attempted so far and provides an interesting case study. The TES detector array is produced using fairly conventional lithographic and micromachining processes, and is then hybridized (indium bump-bonded) to the readout multiplexer (see Fig. 5). Multiplexer fabrication is the most difficult and expensive aspect of the array production.

The superconducting (SQUID-based) TES multiplexing schemes now in use have various limitations in terms of cold power dissipation, multiplex factor, expense and complexity, etc. The simplest solution is to avoid superconducting active electronics altogether, and to use passive frequency–multiplexed superconducting microresonators as detectors.[6] In this "MKID" scheme, the complex readout electronics resides at room temperature (see Fig. 5). Meanwhile, fabrication of the MKID arrays is quite straightforward and the multiplexing is built-in, so bump bonding is unnecessary. A 2304-detector MKID camera is currently under construction for the CSO. Scaling up either TES or MKID technology to the 50-100 kilopixel range represents a significant but not insurmountable technical challenge.

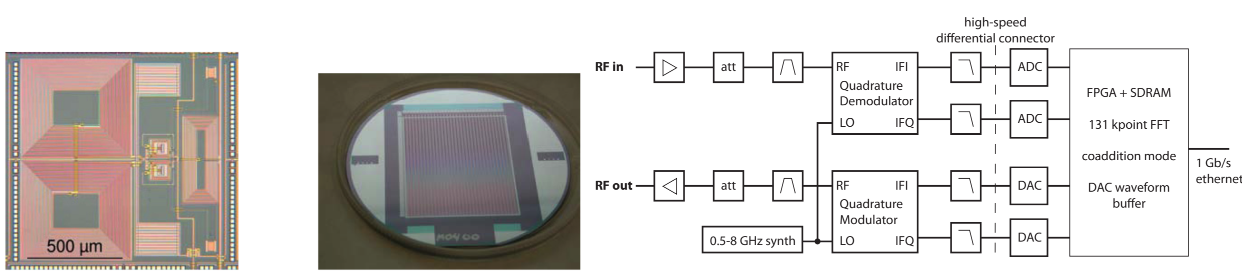

Figure 5: Left: The 32 × 40 SCUBA-2 readout multiplexer is a complex, wafer–scale, custom superconducting integrated circuit. The readout circuitry for each pixel occupies an area around 1 mm^2. Device fabrication involves Nb/Al-oxide/Nb tunnel junctions, 10 lithography levels, and 60 reticles (mask patterns). Credit: Gene Hilton, NIST. Right: A block diagram of the radio-frequency multiplexing electronics being developed for the CSO MKID camera, using mass-produced digital and wireless silicon integrated circuits. The circuitry shown fits on a modest-sized board, dissipates ∼ 30 W, and is capable of reading out > 1000 detectors at ∼$10 per detector.

Table 3: Available Observing Time

Band		Time	Ref.	CCAT (5612 m)			ALMA (5050 m)		
λ	ν	to CL[a]	PWV[b]	Time Available		CL fields[c]	Time Available		CL fields[c]
(μm)	(GHz)	(hr)	(mm)	(hr yr^{-1})	(%)	(yr^{-1})	(hr yr^{-1})	(%)	(yr^{-1})
200	1500	1248	0.26	281	3		84	1	
350	857	0.86	0.47	1936	22	2244	1084	12	1257
620	484	1.14	0.64	716	8	629	723	8	634
740	405	0.43	0.75	639	7	1488	690	8	1607
865	347	0.28	0.86	1223	14	4413	1205	14	4348
1400	214	0.30	1.00	1517	17	5093	1299	15	4361
Total time for PWV $<$ 1.1 mm:				6312	72		5084	58	

[a] Time to reach the confusion limit (CL) – see Table 2.

[b] The reference precipitable water vapor (PWV) is the adopted maximum value for observations in a given wavelength band. Several bands have equivalent thresholds (e.g. 350/450 μm) and for simplicity only one band is listed.

[c] Number of confusion-limited fields per year.

We probably don't have room for this table...

References

[1] CCAT instrumentation workshop, December 2006. Available at http://www.submm.org/mtg/2006/2006-12-pasadena/2006-12-pasadena.html.

[2] Cornell Caltech Atacama Telescope Feasibility/Concept Design Study. Technical report, January 2006. Available at www.submm.org.

[3] Spectroscopy with CCAT: Science and instrumentation opportunities, May 2008. Available at http://www.submm.org/mtg/2008/2008-05-boulder/2008-05-boulder.html.

[4] AW Blain, I Smail, RJ Ivison, JP Kneib, and DT Frayer. Submillimeter galaxies. *Physics Reports-Review Section of Physics Letters*, 369(2):111–176, OCT 2002.

[5] JA Chervenak, KD Irwin, EN Grossman, JM Martinis, CD Reintsema, and ME Huber. Superconducting multiplexer for arrays of transition edge sensors. *Applied Physics Letters*, 74(26):4043–4045, JUN 28 1999.

[6] PK Day, HG Leduc, A Goldin, T Vayonakis, BA Mazin, S Kumar, J Gao, and J Zmuidzinas. Antenna-coupled microwave kinetic inductance detectors, APR 15 2006. Nuclear Instruments & Methods In Physics Research Section A-Accelerators Spectrometers Detectors and Associated Equipment.

[7] P.M. Downey, A.D. Jeffries, S.S. Meyer, R. Weiss, F.J. Bachner, J.P. Donnely, W.T. Lindley, R.W. Mountain, and D.J. Silversmith. Monolithic silicon bolometers. *Applied Optics*, 23(6):910–914, 1984.

[8] C. Groppi, C. Walker, C. Kulesa, D. Golish, J. Kloosterman, P. Pütz, S. Weinreb, T. Kuiper, J. Kooi, G. Jones, J. Bardin, H. Mani, A. Lichtenberger, T. Cecil, A. Hedden, and G. Narayanan. SuperCam: a 64 pixel heterodyne imaging spectrometer. In *Society of Photo-Optical Instrumentation Engineers (SPIE) Conference Series*, volume 7020 of *Society of Photo-Optical Instrumentation Engineers (SPIE) Conference Series*, August 2008.

[9] Todd Hunter, Melinda Mello, Fred Schwab, Brian Mason, Frank Ghigo, Bojan Nikolic, Simon Dicker, and Phil Korngut. Removal of daytime thermal deformations in the GBT active surface via out-of-focus holography. Presentation at 2009 URSI National Radio Science Meeting, Boulder CO, January 2009. Available at www.astro.caltech.edu/USNC-URSI-J/Boulder%202009%20presentations/Wednesday%20PM/Hunter_URSI_09.pdf.

[10] K.D. Irwin. An application of electrothermal feedback for high-resolution cryogenic particle-detection. *Applied Physics Letters*, 66(15):1998–2000, APR 10 1995.

[11] D. MacDonald, D. Woody, C. M. Bradford, R. Chamberlin, M. Dragovan, P. Goldsmith, S. Radford, T. Sebring, and J. Zmuidzinas. Cornell Caltech Atacama Telescope primary mirror surface sensing and controllability. In *Society of Photo-Optical Instrumentation Engineers (SPIE) Conference Series*, volume 7012 of *Society of Photo-Optical Instrumentation Engineers (SPIE) Conference Series*, August 2008.

[12] C Papovich, H Dole, E Egami, E Le Floc'h, PG Perez-Gonzalez, A Alonso-Herrero, L Bai, CA Beichman, M Blaylock, CW Engelbracht, KD Gordon, DC Hines, KA Misselt, JE Morrison, J Mould, J Muzerolle, G Neugebauer, PL Richards, GH Rieke, MJ Rieke, JR Rigby, KYL Su, and ET Young. The 24 micron source counts in deep Spitzer Space Telescope surveys. *Astrophysical Journal Supplement Series*, 154(1):70–74, sep 2004.

[13] S. J. E. Radford, R. Giovanelli, G. E. Gull, and C. P. Henderson. Submillimeter observing conditions on Cerro Chajnantor. In *Society of Photo-Optical Instrumentation Engineers (SPIE) Conference Series*, volume 7012 of *Society of Photo-Optical Instrumentation Engineers (SPIE) Conference Series*, August 2008.

[14] G. J. Stacey, S. R. Golwala, C. M. Bradford, C. D. Dowell, G. Cortes-Medellin, T. Nikola, J. Zmuidzinas, T. L. Herter, S. J. Radford, J. P. Lloyd, A. W. Blain, R. L. Brown, D. B. Campbell, R. Giovanelli, P. Goldsmith, P. M. Harvey, C. Henderson, W. D. Langer, T. G. Phillips, A. C. S. Readhead, and D. P. Woody. Instrumentation for the CCAT Telescope. In *Society of Photo-Optical Instrumentation Engineers (SPIE) Conference Series*, volume 6275 of *Society of Photo-Optical Instrumentation Engineers (SPIE) Conference Series*, July 2006.

[15] S. Von Hoerner. Design of large steerable antennas. *Astronomical Journal*, 72(1):35–&, 1967.

[16] R. W. Wilson, M. Devlin, K.-Y. Lo, M. Mountain, P. Napier, J. Nelson, and A. Russell. Report of the Review Committee: Cornell Caltech Atacama Telescope Feasibility/Concept Design Study. Technical report, March 2006. Available at www.submm.org.

[17] D. Woody, D. MacDonald, M. Bradford, R. Chamberlin, M. Dragovan, P. Goldsmith, J. Lamb, S. Radford, and J. Zmuidzinas. Panel options for large precision radio telescopes. In *Society of Photo-Optical Instrumentation Engineers (SPIE) Conference Series*, volume 7018 of *Society of Photo-Optical Instrumentation Engineers (SPIE) Conference Series*, July 2008.

[18] J Yoon, J Clarke, JM Gildemeister, AT Lee, MJ Myers, PL Richards, and JT Skidmore. Single superconducting quantum interference device multiplexer for arrays of low-temperature sensors. *Applied Physics Letters*, 78(3):371–373, JAN 15 2001.